Journal of Solid State Chemistry **152,** 435–440 (2000)
doi:10.1006/jssc.2000.8701, available online at http://www.idealibrary.com on IDEAL®

Crystal Growth and Structural Investigations of the Oxygen Ion Conductor $BaBi_3O_{5.5}$

Saeid Esmaeilzadeh,* Pedro Berastegui,* Jekabs Grins,* and Håkan Rundlöf†

*Department of Inorganic Chemistry, Arrhenius Laboratory, Stockholm University, SE-106 91 Stockholm, Sweden; and
†Studsvik Neutron Research Laboratory, SE-611 82 Nyköping, Sweden

Received December 27, 1999; in revised form February 29, 2000; accepted March 3, 2000

Large single crystals of the oxygen ion conductor $BaBi_3O_{5.5}$ have been obtained, and its structure was investigated by single-crystal X-ray diffraction (XRD) and neutron diffraction (ND), electron diffraction, and high-resolution electron microscopy (HREM). The basic three-dimensional structure was refined, using single crystal ND data, in space group $Im\bar{3}m$ to a weighted R value of 5.3% for 17 unique reflections, with Ba and Bi atoms statistically distributed on the 2(a) sites (0, 0, 0) and the O atoms on the 6(b) sites ($\frac{1}{2}$, 0, 0) with a refined occupancy of 36(1)%. The refined thermal-displacement parameters for the O atoms are highly anisotropic, with $U_{11} = U_{22} = 0.27(1)$ and $U_{33} = 0.082(7)$ Å^2. In addition, the structure is incommensurately modulated with the systematic absence conditions $F\langle hklmnp\rangle = 0$ unless $h + k + l = 2j$ and $m + n + p = 2j$, implying the six-dimensional superspace group $P{:}Im\bar{3}m{:}Im\bar{3}m$, with $a = 4.3798(2)$ Å and modulation vectors $q_1 = [\alpha, 0, 0]^*$, $q_2 = [0, \alpha, 0]^*$, and $q_3 = [0, 0, \alpha]^*$ with $\alpha = 0.3835(1)$. The diffraction data and the HREM images indicate that the modulation is predominantly occuptional. The satellite reflections have comparable intensities in powder XRD and ND patterns, indicating furthermore that the modulation originates from ordering of both O atoms/vacancies and metal atoms. © 2000 Academic Press

Key Words: **barium bismuth oxide; crystal growth; neutron diffraction; three-dimensional modulation; oxygen ion conductor.**

INTRODUCTION

Many bismuth-based oxides are interesting materials owing to their high oxygen-ion conductivity. Ternary bismuth oxides with high bismuth contents have been extensively studied by different scientific groups for many years, but many questions still remain unanswered concerning the mechanism of oxygen-ion conduction and the variety of the structures. Many interesting experiments become possible if single crystals of these phases can be grown, with sizes of a few mm, that are of great importance for a clarification of the conductivity mechanisms, including single crystal neutron diffraction (ND) and crystallographically oriented ionic-conductivity measurements.

A large number of phases with fluorite-related crystal structures can be obtained by adding to the Bi_2O_3 matrix metal oxides with higher-valent cations such as Nb^{5+}, Ta^{5+}, Mo^{6+}, and W^{6+} (1). Their structures are frequently commensurately or incommensurately modulated and/or demonstrate complex and unique orderings. Ternary bismuth-rich oxides containing lower-valent cations, on the other hand, are often found to crystallize with a body-centered cubic (bcc) arrangement of cations (2–6). For lower bismuth contents perovskite related phases are found. It is notable that some of these, including the perovskite $Ba_{0.6}K_{0.4}BiO_3$, are superconductors at temperatures near 30 K (7), and that they do not contain copper. Three similar structure types have been recognized for the bismuth-rich phases. They all have the cubic $Im\bar{3}m$ symmetry, $a \approx 4.4$ Å, and the cations statistically distributed on the 2(b) sites (0, 0, 0). The three structure types differ in the positions of the O atoms. Two of them are anti-α-AgI-type structures and are adopted, e.g., by $Cd_{0.21}Bi_{0.79}O_{1.395}$ (2), in which the O atoms are statistically distributed over the 12(d) sites ($\frac{1}{4}$, 0, $\frac{1}{2}$), and by $Ca_{0.4}Bi_{0.6}O_{1.3}$ (8), in which the O atoms are distributed over 24(g) sites (x, 0, $\frac{1}{2}$), with $x = 0.322(1)$. The third kind of structure can be regarded as related to the perovskite type, with the O atoms distributed over the 6(b) sites ($\frac{1}{2}$, 0, $\frac{1}{2}$). It is found for $BaBi_3O_{5.5}$ (5, 6), which allegedly also has two further modifications (5). It can be noted that the O atoms in all three structure types are located on (x, 0, $\frac{1}{2}$) positions with x varying between $\frac{1}{4}$ and $\frac{1}{2}$. The $BaBi_3O_{5.5}$ compound is an oxygen-ion conductor with an activation energy of 0.90 eV and $\sigma = 10^{-3}\,\Omega^{-1}\,cm^{-1}$ at 673 K (6). Its structure has been studied by powder X-ray diffraction (XRD) (5), electron diffraction (ED) (5), and powder ND (6). In addition to the average structure there is an incommensurate modulation present with three modulation vectors $q_i \approx \langle 0.38, 0, 0\rangle^*$ parallel with the cubic unit cell axes.

This work consists of a reinvestigation of the average structure of $BaBi_3O_{5.5}$ using single-crystal XRD and ND data. The structure modulations have also been investigated

0022-4596/00 $35.00

by ED and high-resolution electron microscopy (HREM), and a superspace-group symmetry for the modulated six-dimensional structure has been deduced.

EXPERIMENTAL

A homogenous red powder was obtained by reacting $Ba(NO_3)_2$ and Bi_2O_3 at 750°C for 2×24 h. The obtained $BaBi_3O_{5.5}$ powder was then heated in a Pt crucible to 950°C, cooled to 700°C at a rate of 3°C/h and then quenched to room temperature. The quenched $BaBi_3O_{5.5}$ material was crushed and found to contain single crystals with sizes up to 30 mm^3, suitable for single-crystal ND experiments.

A focusing Guinier–Hägg camera with Cu$K\alpha_1$ radiation and Si as internal standard was used for phase identification and determination of the unit-cell parameter and modulation vector. The films were evaluated with a scanner system (9).

The Ba/Bi composition of the sample was confirmed by energy-dispersive X-ray (EDX) analysis, using a LINK AN10000 system mounted in a JEOL 820 scanning electron microscope. The EDX point analyses were made on single-crystal surfaces with a statistical error in each analysis of ca. 0.7 at. %.

A JEOL 2000 FX transmission electron microscope operated with an acceleration voltage of 200 kV was used for collecting ED patterns. The HREM images were recorded with a JEOL 3010 transmission electron microscope operated with an acceleration voltage of 300 kV and with an optimal resolution of 1.7 Å. The investigated specimens were crushed, dispersed in butanol, and the dispersions then transferred onto holey carbon-coated copper grids.

A STOE single-crystal X-ray diffractometer with an image-plate detector system, a Siemens rotating anode, and Mo$K\alpha$ radiation was used to record single-crystal XRD data. The distance between the crystal and the image plate was set to 60 mm, corresponding to a 2θ range up to 56° and d values ≥ 0.75 Å.

A four-circle single crystal diffractometer at the Studsvik Neutron Research Laboratory was used for collecting the ND data. A beam of neutrons with the wavelength 1.21 Å was used, monochromatized with a Cu (220) crystal, and the 2θ range up to 90° was covered.

RESULTS

Millimeter-size single crystals were obtained from the slowly cooled $BaBi_3O_{5.5}$ melt. The metal composition of the crystals was determined, by 10 EDX point analyses, to be 24.8(5)% Ba and 75.2(5)% Bi. The unit-cell parameter and the length of the modulation vectors were determined from Guinier–Hägg film data, using nonlinear least-squares refinement, to be $a = 4.3798(2)$ Å and $\alpha = 0.3835(1)$.

Electron Diffraction

Indexed electron diffraction patterns (EDPs) with zone axes $\langle 100 \rangle$ and $\langle 110 \rangle$ are shown in Figs. 1a and 1b, respectively, and an illustration of the $\langle 100 \rangle$ EDP in Fig. 1c. The $\langle 100 \rangle$ EDP should be compared with the observed intensity distribution in the $hk0$ plane of the single-crystal XRD data, shown in Fig. 1d.

The EDPs show strong bcc-type reflections, i.e., reflections from the basic I-centered unit cell, and in addition incommensurate satellite reflections. Six diffraction indices have to be used for indexing the entire patterns, three representing the basic commensurate vectors and three used for indexing the satellite reflections. Cross-term reflections with indices of the type $hklmnp$ with $m \neq 0$, $n \neq 0$, and $p \neq 0$ show that the structure is truly a six-dimensional one and that six indices are thus required. The systematic absence conditions are found to be $F\langle hklmnp \rangle = 0$ unless $h + k + l = 2j$ and $m + n + p = 2j$, which implies a six-dimensional superspace group of the type $P : Im\bar{3}m : Im\bar{3}m$, with the modulation vectors $q_i \approx \langle 0.38, 0, 0 \rangle^*$.

The relative intensities of the satellite reflections in the EDPs, compared to the intensities of the basic reflections, are observed to decrease with increasing 2θ angle. This is also evident, even more clearly, in the single-crystal XRD data (Fig. 1d), which have a much more reliable intensity distribution. This indicates that the atomic modulation waves are predominantly occupational.

High-Resolution Electron Microscopy

An HREM image along the $\langle 100 \rangle$ zone axis is shown in Fig. 2a. The image distinctly shows the presence of ordering additional to that of the basic bcc structure. To remove noise from the periodic pattern the data were Fourier transformed and filtered, using the program CRISP (10). The Fourier transform of the HREM image is given in Fig. 2b. In addition to basic bcc-type reflections of the $hkl000$ type it also contains satellite reflections, e.g., $0000\bar{2}0$. The Fourier transform demonstrates, through the presence of strong satellite reflections, that the HREM image contains information about the modulations. The Fourier-filtered HREM image given in Fig. 2c was obtained by using spatial frequencies corresponding to both bcc type and satellite reflections in the Fourier transform in Fig. 2b. The filtered HREM image reveals not only a bcc pattern but also a quite strong contrast generated by the modulation waves. The appearance of the contrast suggests that the modulation is predominantly occupational (as the diffraction patterns also indicate). Some kind of clustering of atoms and/or O atom vacancies would accordingly correspond to the lighter and darker groups of atoms seen.

HREM images of all of the investigated crystallites along the $\langle 100 \rangle$ zone axis revealed two axial wave vectors

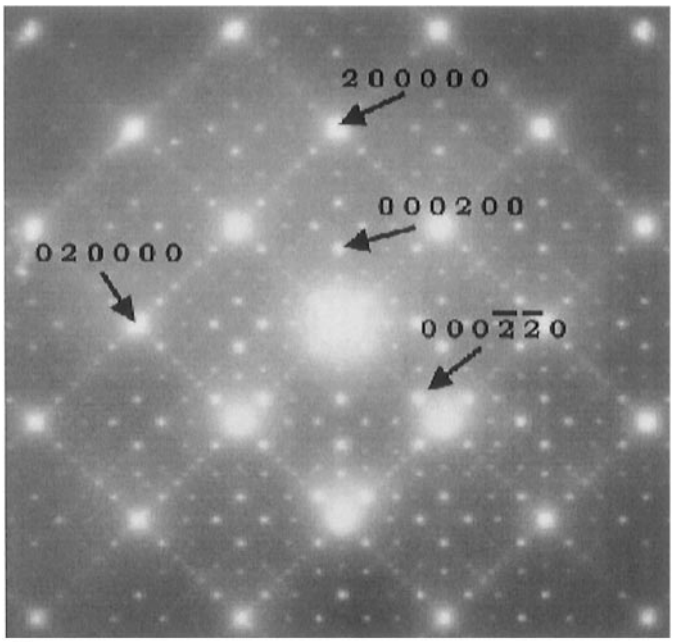

(a)

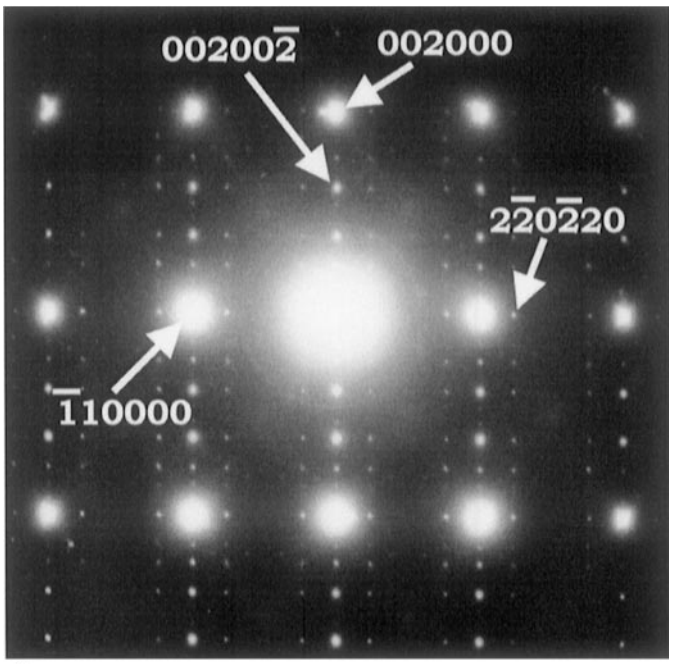

(b)

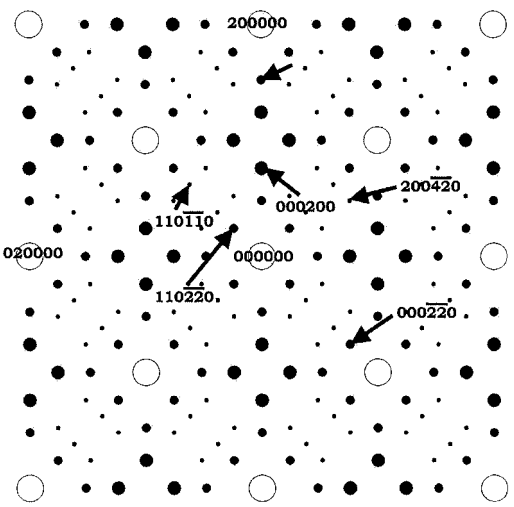

(c)

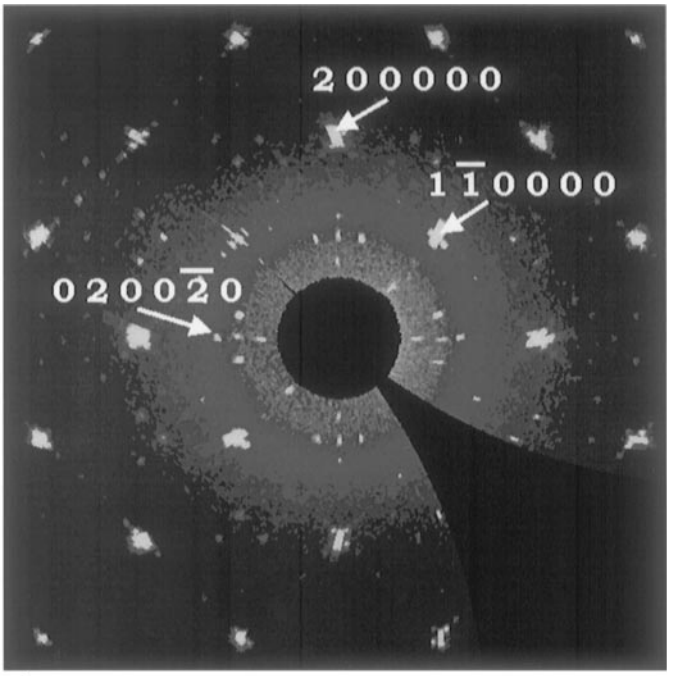

(d)

FIG. 1. EDPs of $BaBi_3O_{5.5}$ with zone axes (a) ⟨100⟩ and (b) ⟨110⟩. (c) A schematic illustration of the ⟨100⟩ EDP. Basic bcc and satellite reflections are represented by open and filled circles, respectively. (d) The intensity distribution in the *hk*0 plane for the single crystal XRD data.

in addition to the basic bcc pattern. A large number of different crystals were studied and the reasonable conclusion has therefore been that the modulation functions extend along all three cubic axes and that the modulated structure is thus properly described by a six-dimensional unit cell.

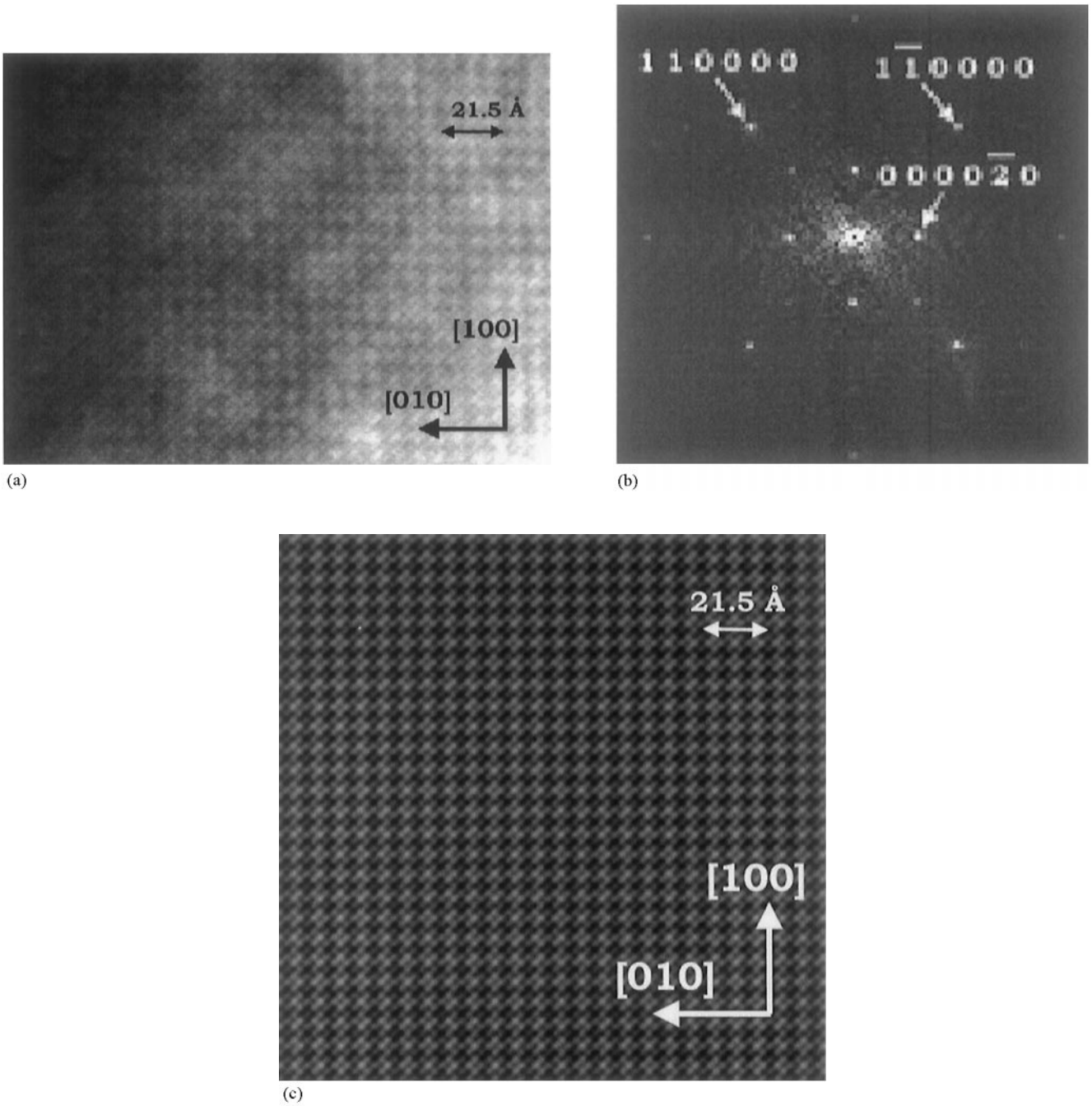

FIG. 2. (a) An HREM image of $BaBi_3O_{5.5}$ along the $\langle 100 \rangle$ zone axis. (b) A Fourier transform of the HREM image. (c) A Fourier-filtered HREM image showing only the periodic patterns that generate the "Bragg peaks" in the fourier transform in (b).

Neutron Diffraction

Single-crystal ND data, collected at the Studsvik Neutron Research Laboratory, were used for refinement of the average commensurate structure. The ND data are here considered to be superior to XRD data for investigation of the title compound, since a great deal of disorder can be expected in the oxygen matrix of its structure.

Data were collected for 67 basic bcc reflections, out of which 17 were unique. The structure was refined in the space group $Im\bar{3}m$ with $a = 4.395(4)$ Å. The cations Ba^{2+} and Bi^{3+} were distributed statistically on the 2(*a*) positions

(0, 0, 0) and the O atoms on the 6(*b*) ($\frac{1}{2}$, 0, $\frac{1}{2}$) positions with an occupation of 46%. A total number of four structural parameters were refined: an isotropic temperature parameter for the metal site ($U = 0.067(1)$ Å^2), two thermal and/or static displacement parameters for the O atoms ($U_{11} = U_{22} = 0.27(1)$ and $U_{33} = 0.082(7)$ Å^2), and site occupancy factor (SOF) for the O atom site, with a refined value of 36(1)%. The large and highly anisotropic thermal displacement parameters for the O atoms indicate that they are highly disordered in planes parallel with ⟨100⟩. The refined SOF of 36(1)% for the O atoms is significantly lower than the nominal one of 46%. The disparity shows that the disorder at or near the O atom 6(*b*) sites can only approximately be described by the model used. Attempts to distribute the O atoms on more general sites, e.g., 12(*d*), yielded no improvements and difference Fourier maps did not exhibit notable residual densities.

Structure Description

The average structure can be described as two interpenetrating cubic ReO_3-type structures with 64% vacancies on the O atom sites. The metal atoms *M* have a bcc arrangement with a *M*–*M* distance of 3.7930(2) Å and a statistical distribution of Ba and Bi atoms in the average structure model. The O sites ($\frac{1}{2}$, 0, $\frac{1}{2}$) are coordinated by an octahedron of four adjacent O sites forming a square and two apical *M* atom sites. The *M*–O and O–O distance in this $O(O_4M_2)$ octahedron is 2.1899(1) Å. The O atoms are highly anisotropic with displacement ellipsoids shaped as discs compressed in the *M*–O–*M* direction along ⟨100⟩ and elongated in the $O(O_4)$ plane. The thermal-displacement ellipsoids of the *M* and O atoms are illustrated in Fig. 3.

The relation to an anti α-AgI structure may be illustrated using the *M*–O polyhedra in the two structure types as shown in Figs. 4a and 4b. In the $BaBi_3O_{5.5}$ structure (Fig. 4a) each *M* atom is coordinated by six O sites forming regular octahedron, while in anti α-AgI (Fig. 4b) the *M* atoms are coordinated by 24 O at 12(*d*) sites, with partial occupancies, forming a truncated octahedron.

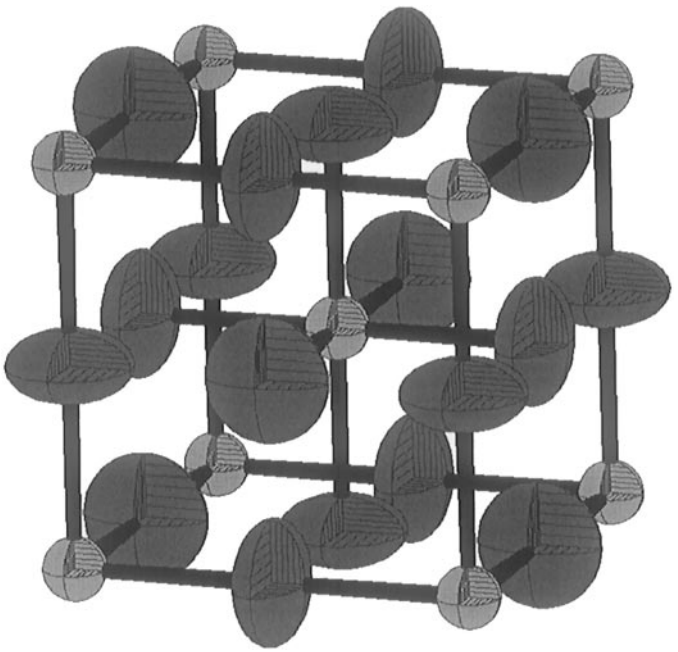

FIG. 3. The average structure of $BaBi_3O_{5.5}$ showing the anisotropic thermal-displacement ellipsoids of the atoms.

DISCUSSION

To obtain more detailed information about the ordering of the O atoms and the vacancies it is necessary to collect ND data on both the basic bcc and the satellite reflections. Such a single crystal ND experiment for $BaBi_3O_{5.5}$ is scheduled. However, the combination of the information obtained in this study for the average structure, using basic bcc type ND reflections, and ED and HREM studies, contribute to the understanding of the local structure.

Our findings may be compared with those from previous investigations (5, 6). The average structure of $BaBi_3O_{5.5}$ has been refined to $R_I = 3.4\%$ from powder ND data (6). The obtained anisotropic displacement factors for the O atoms ($\beta_{11} = \beta_{22} = 0.285(5)$ and $\beta_{33} = 0.067(3)$) are very similar to the ones obtained here from single crystal ND data ($U_{11} = U_{22} = 0.27(1)$ Å^2 and $U_{33} = 0.082(7)$ Å^2). The powder ND data, however, yielded an SOF for the O atoms of 46.2(6)%, in good accordance with the nominal value of 46%, while we obtain a lower value of 36(1)% from the single crystal ND data. With regard to the structure modulations we deduce, on the basis of EDPs and single crystal XRD data, that the correct reflection absence conditions are $F\langle hklmnp\rangle = 0$ unless $h + k + l = 2j$ and $m + n + p = 2j$, implying the superspace-group symmetry $P : Im\bar{3}m : Im3m$, and not $F\langle hklmnp\rangle = 0$ unless $h + k + l + m + n + p = 2j$ as previously suggested (5, 6).

The relative intensities of the satellite reflection are roughly similar in powder XRD and ND data (6), e.g., with intensities of 5 and 12% for $1100\bar{2}0$, respectively. This indicates that the modulation is due to an ordering of both O atoms/vacancies and *M* atoms, quite possibly of the kind proposed in Ref. (6), with two different (local) configurations of a cubic perovskite structure in the crystal. The contrast in the HREM images, where groups of lighter and darker atoms can be distinguished, also indicates a clustering of atoms.

The refined average structure of $BaBi_3O_{5.5}$, with highly anisotropic O atoms, gives some information about the oxygen-ion conduction. Since the displacement ellipsoids of the O atoms are elongated toward the four nearest adjacent O sites and the O vacancy concentration is very high, ca.

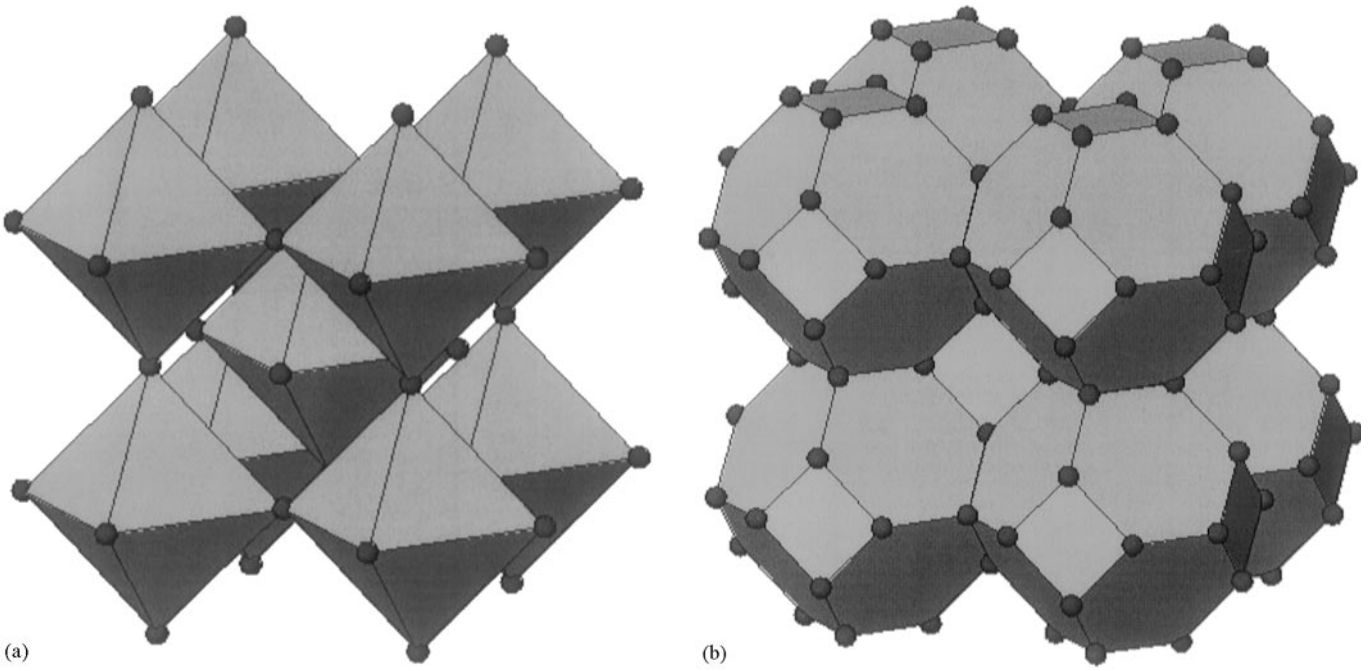

FIG. 4. A comparison between the structure of (a) $BaBi_3O_{5.5}$, illustrated as two interpenetrating ReO_3-type frameworks, and (b) the structure of anti α-AgI, illustrated using the same type of ReO_3 frameworks, but with truncated octahedra.

54%, a probable model for the conduction mechanism involves jumps of oxygen ions to their neighboring vacant sites in the axial $\langle 100 \rangle$ directions. These conduction pathways are visually illustrated in Fig. 5. Ionic-conductivity experiments with single crystals are being planned.

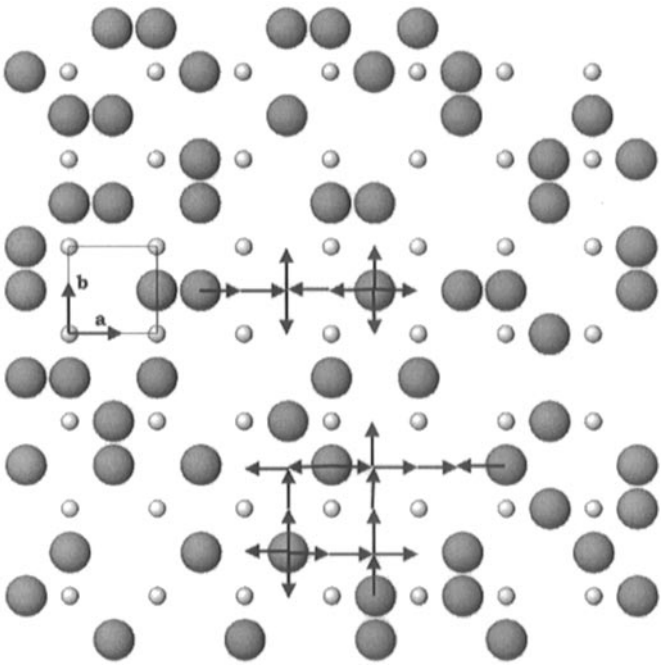

FIG. 5. An illustration of the possible oxygen-ion conduction pathways along $\langle 100 \rangle$.

ACKNOWLEDGMENT

This work has been financially supported by the Swedish Natural Science Foundation.

REFERENCES

1. C. D. Ling, R. L. Withers, S. Schmid, and J. G. Thompson, *J. Solid State Chem.* **37,** 42 (1998).
2. T. Graia, P. Conflant, G. Nowogrocki, J. C. Boivin, and D. Thomas, *J. Solid State Chem.* **63,** 160 (1986).
3. U. Delicat, K. Gruber, A. Püttner, E. J. Zehnder, and M. Trömel, *J. Solid State Chem.* **102,** 209 (1993).
4. K. Gruber, P. Hofer, M. Trömel, H. Fuess, and M. Pinot, *J. Solid State Chem.* **108,** 250 (1994).
5. F. Abbattista, M. Hervieu, M. Vallino, C. Michel, and B. Raveau, *J. Solid State Chem.* **104,** 338 (1993).
6. C. Michel, D. Pelloquin, M. Hervieu, B. Raveau, F. Abbattista, and M. Vallino, *J. Solid State Chem.* **109,** 122 (1994).
7. R. J. Cava, B. Batlogg, J. J. Krajewski, R. C. Farrow, L. W. J. Rupp, A. E. White, K. T. Short, W. F. J. Peck, and T. V. Kometani, *Nature* **332,** 814 (1988).
8. K. Gruber, P. Hofer, M. Trömel, H. Fuess, and M. Pinot, *J. Solid State Chem.* **108,** 250 (1994).
9. K. E. Johansson, T. Palm, and P.-E. Werner, *J. Phys. E* **13,** 1289 (1980).
10. S. Hovmöller, *Ultramicroscopy* **41,** 121 (1992).